


# Characterization of postsynaptic calcium signals in the pyramidal neurons of anterior cingulate cortex

Molecular Pain  
Volume 13: 1–13  
© The Author(s) 2017  
Reprints and permissions:  
sagepub.com/journalsPermissions.nav  
DOI: 10.1177/1744806917719847  
journals.sagepub.com/home/mpx  


Xu-Hui Li<sup>1</sup>, Qian Song<sup>1</sup>, Tao Chen<sup>1,2</sup> and Min Zhuo<sup>1,3</sup>

## Abstract

Calcium signaling is critical for synaptic transmission and plasticity. N-methyl-D-aspartic acid (NMDA) receptors play a key role in synaptic potentiation in the anterior cingulate cortex. Most previous studies of calcium signaling focus on hippocampal neurons, little is known about the activity-induced calcium signals in the anterior cingulate cortex. In the present study, we show that NMDA receptor-mediated postsynaptic calcium signals induced by different synaptic stimulation in anterior cingulate cortex pyramidal neurons. Single and multi-action potentials evoked significant suprathreshold  $\text{Ca}^{2+}$  increases in somas and spines. Both NMDA receptors and voltage-gated calcium channels contributed to this increase. Postsynaptic  $\text{Ca}^{2+}$  signals were induced by puff-application of glutamate, and a NMDA receptor antagonist AP5 blocked these signals in both somas and spines. Finally, long-term potentiation inducing protocols triggered postsynaptic  $\text{Ca}^{2+}$  influx, and these influx were NMDA receptor dependent. Our results provide the first study of calcium signals in the anterior cingulate cortex and demonstrate that NMDA receptors play important roles in postsynaptic calcium signals in anterior cingulate cortex pyramidal neurons.

## Keywords

Synaptic plasticity, NMDA receptors, two-photon microscopy, calcium imaging, long-term potentiation, anterior cingulate cortex

Date received: 6 April 2017; revised: 5 June 2017; accepted: 12 June 2017

## Introduction

Synaptic long-term potentiation (LTP) is a key cellular mechanism for long-term changes taking place in both physiological and pathological conditions in mammalian brains.<sup>1–3</sup> Calcium ( $\text{Ca}^{2+}$ )-stimulated signaling pathways, including adenylyl cyclases, cyclic adenosine monophosphate protein kinase A pathways, and calmodulin-dependent protein kinases, are critical for LTP.<sup>4–7</sup> LTP-related calcium signalings have been studied in different regions of the brain such as the hippocampus<sup>8–10</sup> and medial prefrontal cortex.<sup>11,12</sup> In the hippocampus, previous studies show that voltage-gated calcium channels (VGCCs) and N-methyl-D-aspartic acid (NMDA) receptors are two major players for the  $\text{Ca}^{2+}$  influx.<sup>13–15</sup> Activation of postsynaptic NMDA receptors contributes to postsynaptic calcium influx that is essential for triggering LTP.<sup>10,16–19</sup>

Anterior cingulate cortex (ACC) is a critical cortical region for pain perception and emotion regulation.<sup>1,2,20</sup>

LTP is a key form of synaptic plasticity in ACC synapses that plays important roles in physiological and pathological pain.<sup>21–24</sup>  $\text{Ca}^{2+}$  ions trigger a series of biochemical cascades that contribute to the induction of LTP in the ACC.<sup>7,25</sup> Postsynaptic injection of BAPTA completely blocks the induction of LTP, indicating the

<sup>1</sup>Center for Neuron and Disease, Frontier Institutes of Science and Technology, Xi'an Jiaotong University, Xi'an, China

<sup>2</sup>Department of Anatomy, K.K. Leung Brain Research Center, Fourth Military Medical University, Xi'an, China

<sup>3</sup>Department of Physiology, Faculty of Medicine, University of Toronto, Toronto, ON, Canada

## Corresponding authors:

Min Zhuo, Department of Physiology, Faculty of Medicine, University of Toronto, Medical Science Building, Room #3342, 1 King's College Circle, Toronto, ON, Canada, M5S 1A8.

Email: min.zhuo@utoronto.ca

Tao Chen, Department of Anatomy, K.K. Leung Brain Research Center, Fourth Military Medical University, Xi'an, ShaanXi 710032, China.

Email: chtkkl@fmmu.edu.cn



importance of postsynaptic  $\text{Ca}^{2+}$  signaling for ACC LTP.<sup>26</sup> Furthermore, ACC LTP is completely abolished in mice that express mutant CaM (including CaM<sub>12</sub> and CaM<sub>34</sub>, two impaired  $\text{Ca}^{2+}$  binding sites in the N- and C-terminal lobe, respectively).<sup>27</sup> As reported in other central synapses, NMDA receptors are likely the key player for the activity-induced postsynaptic calcium signaling. ACC LTP induced by different protocols is sensitive to the inhibition of NMDA receptors.<sup>7,26,28</sup> However, there is no direct investigation of NMDA receptor-dependent postsynaptic  $\text{Ca}^{2+}$  influx in ACC neurons of adult animals.

In the present study, by combining whole-cell patch recording and two-photon  $\text{Ca}^{2+}$  imaging observation, we recorded postsynaptic  $\text{Ca}^{2+}$  signals that were evoked by different synaptic stimulations in the somas and spines of ACC pyramidal neurons. We found that both NMDA receptors and VGCCs-mediated action potentials (APs) induced suprathreshold  $\text{Ca}^{2+}$  influx. Electrical stimulation and puff-application of glutamate (Glu) can induce subthreshold  $\text{Ca}^{2+}$  signals. These subthreshold  $\text{Ca}^{2+}$  signals were decreased by NMDA receptor antagonist AP5. Finally, we found that  $\text{Ca}^{2+}$  influx were increased in induction of LTP by spike-timing, theta-burst stimulation (TBS), and pairing protocols. These increases were NMDA receptor dependent. Our results are the first that directly observed  $\text{Ca}^{2+}$  signals changes in postsynaptic transmission and plasticity in ACC pyramidal neurons.

## Materials and methods

### Animals

Adult male C57BL/6 mice (6–8 weeks old) were used in the all experiments. The mice were purchased from the Experimental Animal Center of Xi'an Jiaotong University. All mice were randomly housed in corncoiled plastic cages under an artificial 12-h light/dark cycle (lights on 9 a.m.–9 p.m.) with food and water provided ad libitum, at least one week before carrying out experiments. All animals were cared for, and experiments were carried out in accordance with the European Community guidelines for the use of experimental animals (86/609/EEC). All performed research protocols were approved by the Ethics Committee of Xi'an Jiaotong University.

### Brain slice preparation

Coronal brain slices (300  $\mu\text{m}$ ) of ACC were prepared using standard methods.<sup>29–31</sup> Briefly, C57BL/6 mice were anesthetized with 1% to 2% isoflurane. The whole brain was quickly removed from the skull and immersed in the oxygenated (95%  $\text{O}_2$  and 5%  $\text{CO}_2$ ),

ice cold cutting solution containing (in mM): 252 sucrose, 2.5 KCl, 6  $\text{MgSO}_4$ , 0.5  $\text{CaCl}_2$ , 25  $\text{NaHCO}_3$ , 1.2  $\text{NaH}_2\text{PO}_4$ , and 10 glucose, pH: 7.3 to 7.4. After cooling for a short time, the whole brain was trimmed for an appropriate part to glue onto the ice-cold stage of a Leica VT1200S Vibratome. Slices were transferred to a submerged recovery chamber with an oxygenated (95%  $\text{O}_2$  and 5%  $\text{CO}_2$ ) artificial cerebrospinal fluid (ACSF) (124 mM NaCl, 4.4 mM KCl, 2 mM  $\text{CaCl}_2$ , 1 mM  $\text{MgSO}_4$ , 25 mM  $\text{NaHCO}_3$ , 1 mM  $\text{NaH}_2\text{PO}_4$ , and 10 mM glucose; pH: 7.3–7.4) and then incubated at room temperature for at least 1 h before recording.

### Dye injection and drug application

For single cell recording, calcium indicator Cal-520 potassium salt (0.2 mM, AAT Bioquest) was added in a recording pipette directly to monitor  $\text{Ca}^{2+}$  signals that were then diluted with the intracellular solution containing Alexa594 potassium salt (20  $\mu\text{M}$ , Invitrogen) to image morphology.<sup>32,33</sup> Cell population loading of calcium indicator was performed as puff-application of dye on the slice surface, Cal-520 acetoxymethyl ester (Cal-520 AM, 0.2 mM, AAT Bioquest). Dye ejection was performed in layer II/III of the ACC at 5 psi for 3 min using a pico-liter injector (PLI-10, Warner Instrument).

All the chemicals and drugs used in this study were obtained from Sigma (St. Louis, MO, USA), except for CNQX (20  $\mu\text{M}$ ), which was purchased from Tocris Cookson (Bristol, UK). All experiments were conducted in the presence of picrotoxin (100  $\mu\text{M}$ ) to block GABA<sub>A</sub> receptor-mediated inhibitory synaptic currents. Drugs were prepared as stock solutions for frozen aliquots at  $-20^\circ\text{C}$ . They were diluted from the stock solution to the final desired concentration in the ACSF before being applied to the perfusion solution. In some experiments (Figures 6 and 7), a pico-liter injector (PLI-10, Warner Instrument) was used to puff-application of Glu (1 mM). Before recording, the drug pipette was moved beside the neuron using a pico-liter injector (PLI-10, Warner Instrument). The tip of the pipette was 50  $\mu\text{m}$  away from the neuron recorded. The pressure and duration of the puffing were 10 psi and 100 ms, respectively.<sup>34</sup>

### Two-photon imaging

Calcium imaging was performed more than 30 min after dye injection to allow diffusion of the dye into the cell. In vitro calcium imaging was performed using a two-photon laser scanning microscope, which consists of a Olympus FV1000-MPE system (side-mounted to a BX61WI microscope) and a pulsed Ti: sapphire laser (MaiTai HP DeepSee, 690–1040 nm wavelength, 2.5 W average power, 100 fs pulse width, 80 MHz repetition rate; New Port Spectra-Physics, Santa Clara, CA,

USA). The laser was focused through a  $\times 40$  water-immersion objective lens (LUMPLFL/IR40XW, NA: 0.8, Olympus), and the average power was set to  $<15$  mW (measured under the objective). Calcium imaging of somas, dendrites, and spines were acquired at 800 nm. Fluorescent signals of Cal-520 and Alexa594 were separated into green and red channels by a dichroic mirror and emission filters (Chroma, Bellows Falls, VT, USA) and detected by a pair of photomultiplier tubes (Hamamatsu, Shizuoka, Japan).

To obtain time series of fluorescent signals from a single soma, images were collected with the following parameters<sup>33,35,36</sup>:  $512 \times 512$  pixel images, digital zoom  $3\times$  with  $\times 40$  objective (NA: 0.8),  $2\text{-}\mu\text{s}$  pixel dwell time,

1500 lines, 2 ms/line for line scan model or  $512 \times 512$  pixel images, digital zoom  $3\times$  with  $\times 40$  objective (NA: 0.8),  $2\text{-}\mu\text{s}$  pixel dwell time, 50 ms/frame for frame scan model, different recording time for different recording frames. For spines images, the parameters of  $512 \times 512$  pixel images, digital zoom  $5\times$  with  $\times 40$  objective (NA: 0.8),  $2\text{-}\mu\text{s}$  pixel dwell time, 50 ms/frame were used, with different recording times for different recording frames;  $512 \times 512$  pixel images, digital zoom  $1\times$  with  $\times 40$  objective (NA: 0.8), 60 frames, 50 ms/frame,  $2\text{-}\mu\text{s}$  pixels well time for cell populations images. Bidirectional scanning and line-scanning models were used to increase scan speed. Each trial was repeated at least three times, and the mean value was collected.

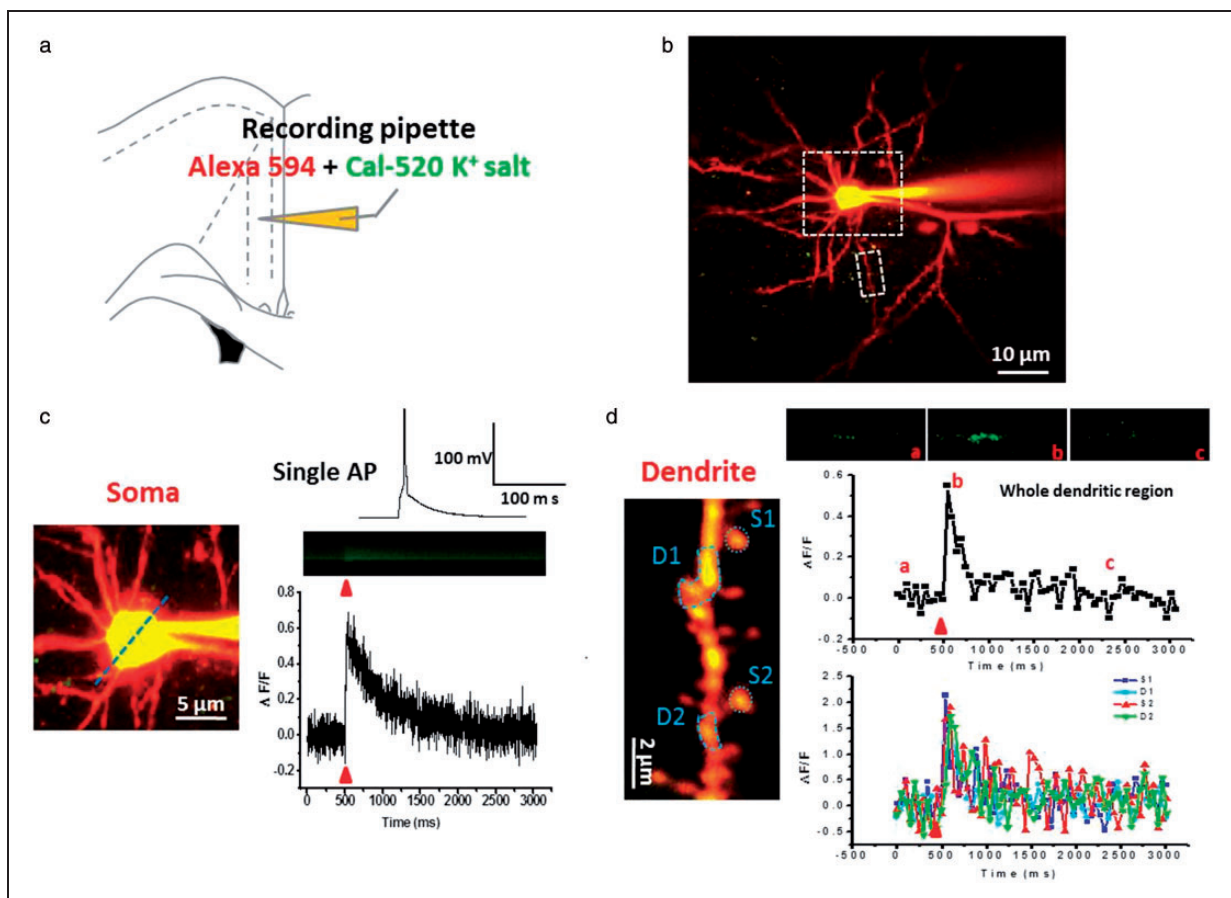


**Figure 1.** Single action potential evoked powerful suprathreshold  $\text{Ca}^{2+}$  signals in soma and dendritic spine of ACC pyramidal neurons. (a) Schematic diagram showing the placement of patch clamp recording and indicator dye in pipette in the layer II/III pyramidal neurons of the ACC. (b) Representative two-photon fluorescent image of patch neuron loading by Alexa 594 and Cal-520  $\text{K}^+$  salt. Larger white dash box represents the soma location in (c), and smaller white dash box represents the dendrite location in (d). (c) Single AP evoked  $\text{Ca}^{2+}$  signals in soma. Upper right: current-clamp trace of single action potential evoked by the current injections of 200 pA (5 ms); middle and lower right: representative calcium transient images (middle) and waveforms of fluorescence change ( $\Delta\text{F}/\text{F}$ ) (down) in response to single AP in soma. (d) Single AP evoked  $\text{Ca}^{2+}$  signals in dendrite. Upper right: representative calcium transient images in response to three time points of single AP in whole dendrite. Middle and lower right: waveforms of fluorescence change ( $\Delta\text{F}/\text{F}$ ) in response to single AP in whole dendrite (middle) and four regions (S1 and S2: spine I and 2; D1 and D2: dendritic region I and 2) (down). In this and following figures: the blue dash line and blue dash circle indicate the position of the line scan and frame scan, respectively. The red arrowheads mark the time points of synaptic stimulation.

### Electrophysiological recordings

Whole-cell recordings were used to load calcium indicator into the cell and electrophysiological recordings simultaneous with calcium imaging. Brain slices were transferred into an immersion-type recording chamber under a two-photon microscope (BX61WI, Olympus) equipped with infrared differential interference contrast optics for visualization. For electrical and calcium imaging recording, slices were perfused with oxygenated and temperature-controlled ACSF ( $30 \pm 1^\circ\text{C}$ ) with TC-324B temperature controller (Warner Instrument). Excitatory postsynaptic currents (EPSCs) were recorded from layer II/III pyramidal neurons in ACC with an Axon 200B amplifier (Molecular Devices). The recording pipettes (3–5 M $\Omega$ ) were filled with a solution containing (in mM) 145 K-gluconate, 5 NaCl, 1 MgCl<sub>2</sub>, 0.2 EGTA,

10 HEPES, 2 Mg-ATP, 0.1 Na<sup>3</sup>-GTP, 10 phosphocreatine disodium, 0.02 Alexa594 potassium salt, and 0.2 Cal-520 potassium salt (AAT Bioquest) (adjusted to pH 7.2 with KOH, 290 mOsmol). The electrical stimulations were delivered by a bipolar tungsten stimulating electrode or a fine-tipped theta stimulation pipette placed in layer V of the ACC. The current-clamp configuration was used recording APs for a single spike (current injections of 200 pA/5 ms) and five spikes at 5, 10, 20, and 50 Hz (current injections five times of 200 pA/5 ms at different frequencies). The resting membrane potential was held at  $-60\text{ mV}$  throughout the experiment. Access resistance was 15 to 30 M $\Omega$  and monitored throughout the experiment. Data were discarded if access resistance changed by 15% during an experiment. Data were filtered at 1 kHz and digitized at 10 kHz using the digidata 1440A.

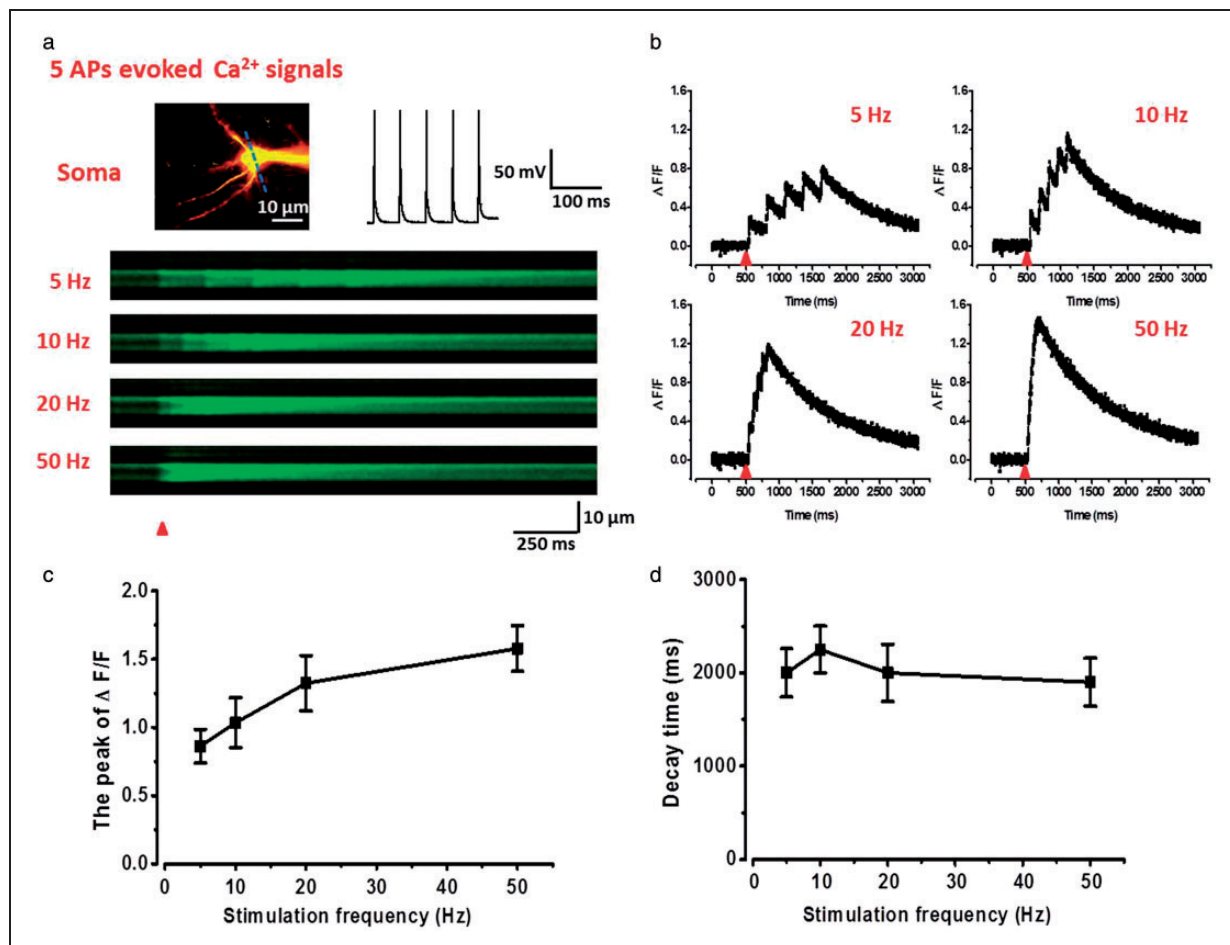


**Figure 2.** Summation properties of multi-APs evoked suprathreshold Ca<sup>2+</sup> signals in soma of ACC pyramidal neurons. (a) Upper left: two-photon fluorescent image of patched neuron. The blue line indicates the position of the line scan. Upper right: representative current-clamp traces of five spikes action potentials evoked by current injection of 200 pA (5 ms). Below: representative calcium transients images in response to five spikes APs trains at 5, 10, 20, and 50 Hz in soma. (b) Representative waveforms of fluorescence changes ( $\Delta\text{F}/\text{F}$ ) in response to five spikes APs at 5, 10, 20, and 50 Hz in soma. (c) Summary results showing the peak values of  $\Delta\text{F}/\text{F}$  to five spikes APs at different frequencies (n = 6). (d) Summary results showing the decay time of  $\Delta\text{F}/\text{F}$  to five spikes APs at different frequencies. APs: action potentials.

Data were collected and analyzed with Clampex and Clampfit 10.2 software (Axon Instruments).

After obtaining stable EPSCs for 10 min, three kinds of LTP induction paradigms were used to induce long-term synaptic plasticity.<sup>26,37</sup> The first involved paired three postsynaptic stimuli that caused three EPSPs (10 ms ahead) with three postsynaptic APs at 30 Hz, paired 15 times every 5 s (named the spike timing protocol). The second involved TBS (five trains of burst with four pulses at 100 Hz), at 200 ms intervals; repeated four times at intervals of 10 s (named the TBS). The third protocol involved paired presynaptic 80 pulses at 2 Hz with postsynaptic depolarization at +30 mV (named the pairing protocol).

### Data analysis

The data are presented as means  $\pm$  SEM. Statistical comparisons between two groups were performed using two-tail paired or unpaired *t* test, one-way analysis of

variance to identify significant differences. In all cases,  $*P < 0.05$  was considered statistically significant.

## Results

Experiments were performed on layer II/III ACC pyramidal neurons in acute slices of mouse brains. We used whole-cell patch recording to obtain electrophysiological data and labeled neurons with the fluorescent dye Alexa 594  $K^+$  salt (20  $\mu$ M) and Cal-520  $K^+$  salt (200  $\mu$ M) via the patch pipette. After allowing 30-min dye diffusion, two-photon microscopy was used to image  $Ca^{2+}$  signals in somas and spines. The spines were selected on basal dendrites 50 to 100  $\mu$ m far away from soma that were clear labeled by dye. Synaptic responses and associated  $Ca^{2+}$  signals were induced by the manners of injection currents, electrical stimulation, puff-application of Glu, and LTP induction. In addition, we also measured the role of NMDA receptors in the calcium transients of different synaptic stimulation in the ACC.

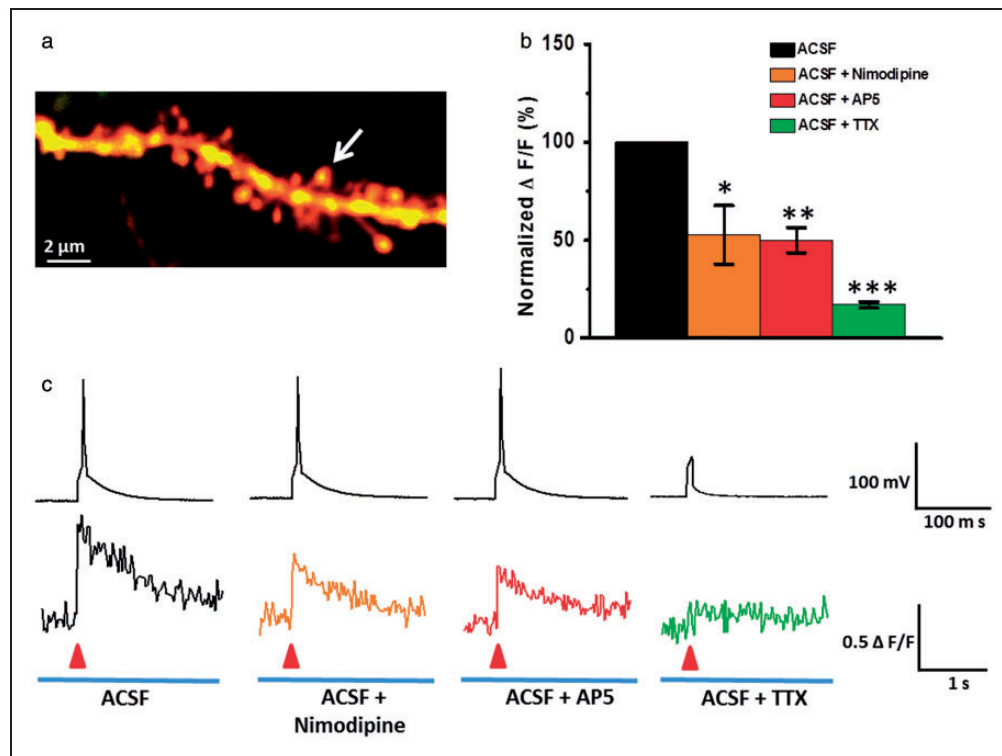


**Figure 3.** NMDA receptors and VGCCs both mediated single AP evoked suprathreshold  $Ca^{2+}$  signal in spine of ACC pyramidal neurons. (a) Representative two-photon fluorescent image of a dendritic segment containing active spine (white arrow). (b) Summary results showing the effects of nimodipine ( $n = 5$ ), AP5 ( $n = 6$ ), and TTX ( $n = 6$ ) on single AP evoked spine  $Ca^{2+}$  signals.  $\Delta F/F$  amplitudes were normalized to control values. (c) Representative current-clamp traces of single AP evoked by current injections of 200 pA (5 ms) (up) and related waveforms of fluorescence changes ( $\Delta F/F$ ) of spines (down) on the perfusion fluid containing ACSF, ACSF + nimodipine, ACSF + AP5, and ACSF + TTX, respectively.  $*P < 0.05$ ,  $**P < 0.01$ , and  $***P < 0.001$ , error bars indicated SEM. The amplitudes of  $Ca^{2+}$  signals ( $\Delta F/F$ ) were normalized to control values. ACSF: artificial cerebrospinal fluid; TTX: tetrodotoxin.

## APs evoked $\text{Ca}^{2+}$ signals

Calcium signals evoked by single AP and multi-APs were recorded in the soma and spine of ACC pyramidal neurons. APs were induced by injecting depolarizing currents through a patch pipette. Two-photon line scans were used to the soma  $\text{Ca}^{2+}$  imaging and frame scans for dendrite and spine imaging. As shown in Figure 1, after 30-min dye diffusion, neuronal morphology was well labeled by Alexa594 (Figure 1(b) to (d)). We observed that soma injection of 200 pA (5 ms) current induced a single AP, which evoked powerful suprathreshold calcium transients in soma ( $\Delta F/F = 0.69 \pm 0.11$ ; Figure 1(c)) and dendrite shafts and spines ( $\Delta F/F = 1.89 \pm 0.23$ ; Figure 1(d)). The peak amplitude of spine  $\text{Ca}^{2+}$  signals were one to three folds greater than that of soma  $\text{Ca}^{2+}$  signals. The calcium signals in the spines head were bigger than that of the dendrite shafts.

We next tested the summation and decay time properties of multi-APs-evoked  $\text{Ca}^{2+}$  signals in the soma of ACC pyramidal neurons. We injected train currents in somas to induce five APs at different frequencies of 5, 10, 20, and 50 Hz. As shown in Figure 2, five APs significantly increased the  $\Delta F/F$  of  $\text{Ca}^{2+}$  signals (5 Hz:  $0.86 \pm 0.12$ ; 10 Hz:  $1.03 \pm 0.18$ ; 20 Hz:  $1.32 \pm 0.25$ ; 50 Hz:  $1.58 \pm 0.27$ ;  $n = 5$ ). Each AP induced an obvious peak of calcium transients, and the  $\Delta F/F$  values had a liner relationship with the AP numbers. The rise time of  $\text{Ca}^{2+}$  signals were related to the stimulation frequencies. However, the decay time was not significantly changed at different stimulation frequencies (Figure 2(d)).

We then examined whether VGCCs and NMDA receptors, the two important channels for  $\text{Ca}^{2+}$  influx,<sup>13</sup> contribute to the AP-induced suprathreshold  $\text{Ca}^{2+}$  signal in the ACC. As shown in Figure 3, a  $\text{Ca}^{2+}$  signal induced by single AP was significantly reduced by

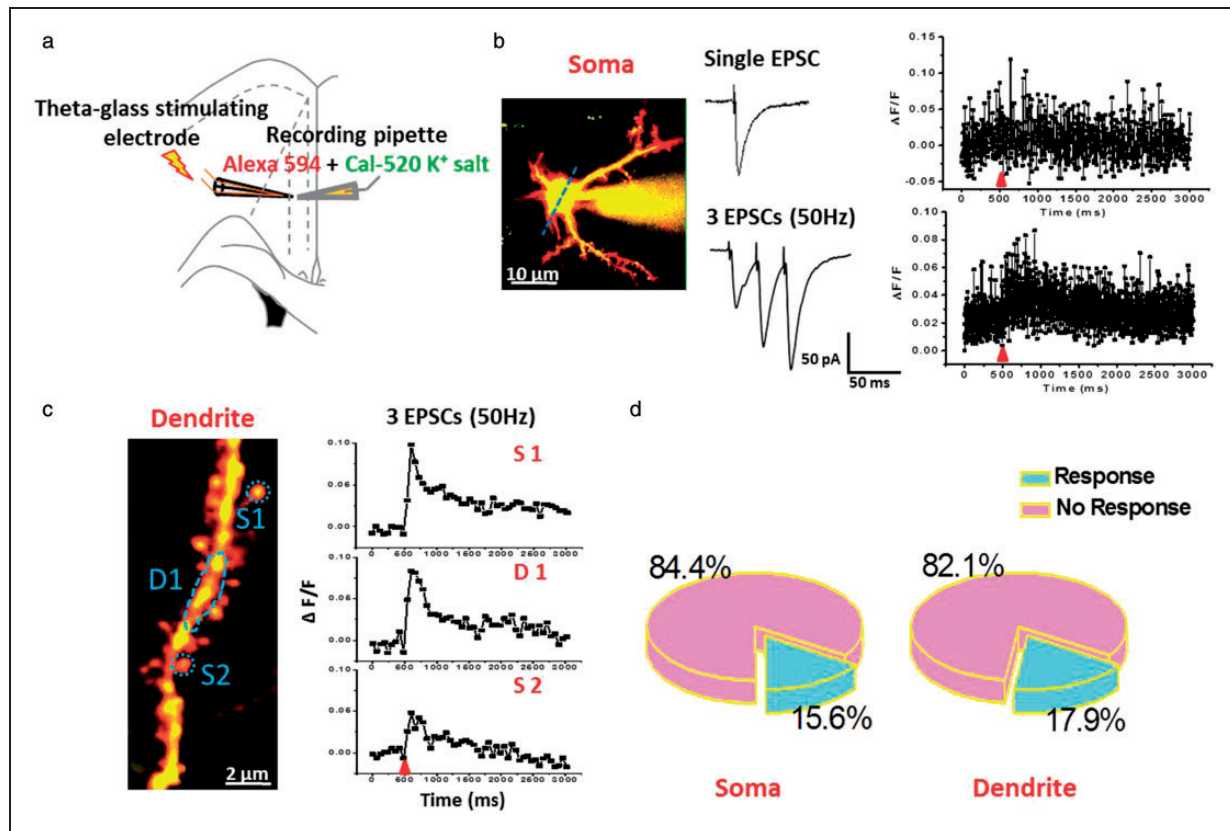


**Figure 4.** Electrical stimulation evoked weak subthreshold  $\text{Ca}^{2+}$  signals in soma and dendritic spine of ACC pyramidal neurons. (a) Schematic diagram showing the placement of stimulating electrode and recording pipette in the layer II/III pyramidal neurons of the ACC. (b) Left: two-photon fluorescent image of patched active neuron. The blue line indicates the position of the line scan. Middle: representative voltage-clamp traces of single EPSC and three traces EPSCs at 50 Hz induced by local stimulation. Right: associated waveforms of fluorescence change ( $\Delta F/F$ ) in response to single EPSC and three traces EPSCs at 50 Hz in soma. (c) Left: two-photon fluorescent image of dendritic segment containing active spines. Right: waveforms of fluorescence change ( $\Delta F/F$ ) in response to three traces EPSCs at 50 Hz for three active regions (S1: spine1; D1: dendritic region1, and S2: spine2). (d) Pie graph summarizing the active ratio of evoked  $\text{Ca}^{2+}$  singles in soma ( $n = 32$ ) and dendrite containing active spines ( $n = 28$ ) after three traces EPSCs at 50 Hz stimulation. EPSCs: excitatory postsynaptic currents.

VGCCs inhibitor nimodipine (10  $\mu\text{M}$ ) (ACSF:  $\Delta F/F = 0.54 \pm 0.11$ ; ACSF + nimodipine:  $\Delta F/F = 0.28 \pm 0.08$ ,  $P < 0.05$ ,  $n = 6$ ). This finding indicates that VGCCs mediate suprathreshold  $\text{Ca}^{2+}$  signals in ACC. NMDA receptors antagonist AP5 (50  $\mu\text{M}$ ) also reduced the  $\text{Ca}^{2+}$  influx (ACSF:  $\Delta F/F = 0.52 \pm 0.08$ ; ACSF + AP5:  $\Delta F/F = 0.23 \pm 0.03$ ,  $P < 0.01$ ,  $n = 6$ ). Our present results show that NMDA receptors also play important roles for AP-evoked suprathreshold  $\text{Ca}^{2+}$  signals in the ACC. To confirm the role of AP, we applied tetrodotoxin (TTX) to block AP. Application of TTX (1  $\mu\text{M}$ ) almost completely blocked the AP-induced  $\text{Ca}^{2+}$  signals (ACSF:  $\Delta F/F = 0.51 \pm 0.10$ ; ACSF + TTX:  $\Delta F/F = 0.08 \pm 0.01$ ,  $P < 0.001$ ,  $n = 6$ ). These results suggest that AP-evoked suprathreshold calcium transients are both mediated by VGCCs and NMDA receptors in spines of ACC pyramidal neurons in mice.

### Weak $\text{Ca}^{2+}$ signals induced by synaptic stimulation

Postsynaptic calcium influx can be induced by subthreshold synaptic stimulation.<sup>17,38</sup> In the present study, we

decided to use a fine-tipped theta-glass bipolar stimulation pipette positioned at 10 to 20  $\mu\text{m}$  to deliver focal electrical stimulation that avoided the production of AP. As shown in Figure 4, although single shock stimulation induced evoked excitatory postsynaptic current (eEPSC), the  $\text{Ca}^{2+}$  signal was not steadily detectable in many somas and spines. In the subsequent study, we performed repetitive electrical stimulation at 50 Hz for three traces in somas and spines (Figure 4(b) and (c)). We found that this stimulation also induced weak calcium signals in somas (15.6%,  $n = 5$  responses/36 in totals) and spines (17.9%,  $n = 5$  responses/28 in totals). These results are similar with those reported before in hippocampal neurons.<sup>17</sup>

To further test the subthreshold synaptic transmission-induced  $\text{Ca}^{2+}$  response, we then incubated ACC slices with acetoxymethyl ester derivative indicator (Cal-520 AM), a membrane permeable dye, for monitoring multi-cell calcium signals. Bipolar tungsten stimulating electrode was used to induce five traces stimulation at different frequencies (5, 10, 20, and 50 Hz) (Figure 5). We found that electrical stimulation at different frequencies evoked weak  $\text{Ca}^{2+}$  signals (Figure 5(b)). However,

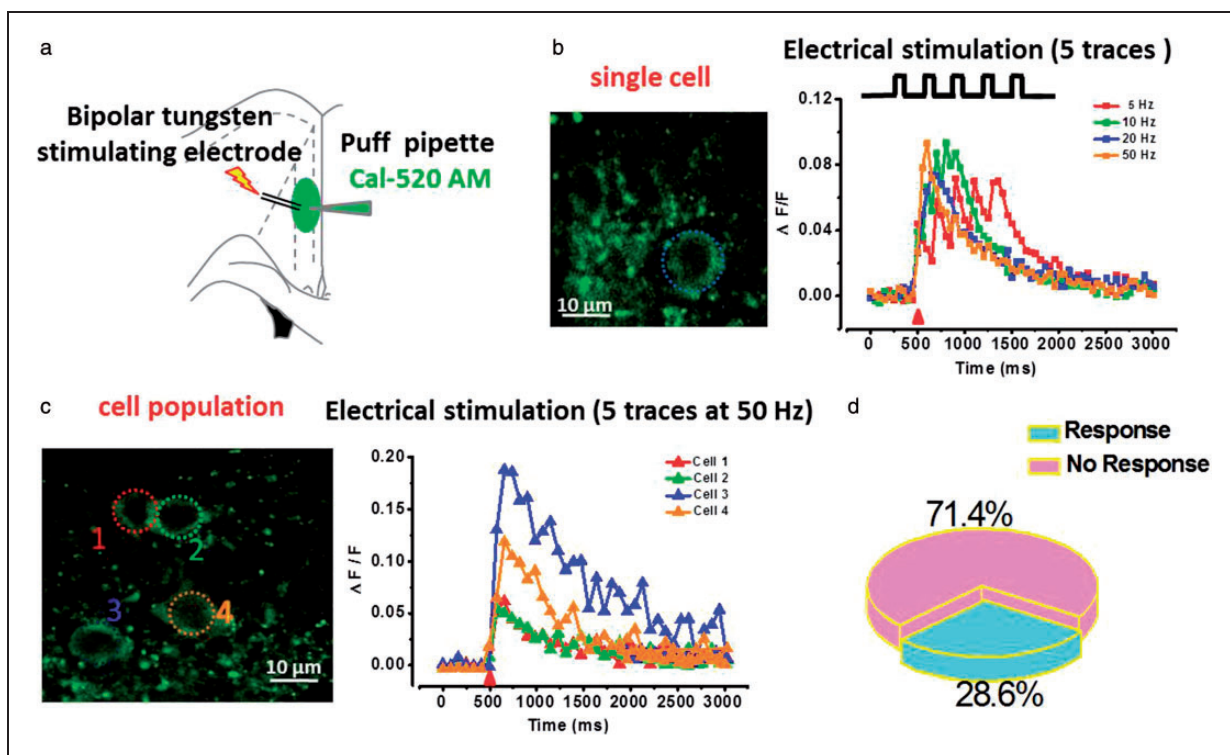


**Figure 5.** Repetitive electrical stimulation evoked  $\text{Ca}^{2+}$  signals in cell population after bolus loading of Cal-520 AM in ACC pyramidal neurons. (a) Schematic diagram showing the placement of stimulating electrode and puffing pipette in the layer II/III pyramidal neurons of ACC. (b) Left: two-photon fluorescent image of puff-application of calcium indicator Cal-520 AM (200  $\mu\text{M}$ ). The blue dash circle indicates the position of the frame scan: Right, waveforms of fluorescence changes ( $\Delta F/F$ ) in response to five traces at 5, 10, 20, and 50 Hz in single cell. (c) Left: representative fluorescent image of cell population showing the soma of active neurons. Right: waveforms of fluorescence changes ( $\Delta F/F$ ) in response to five traces at 50 Hz in four active cells. (d) Pie graph summarizing the active ratio of evoked  $\text{Ca}^{2+}$  signals in cell population ( $n = 42$ ) after five traces at 50 Hz electrical stimulation.

similar to the focal stimulation results, only a few parts of the neurons showed increased  $\text{Ca}^{2+}$  waves (28.6%,  $n=12$  responses/42 in totals), even at 50 Hz stimulation (Figure 5(c) and (d)). In addition, some soma  $\text{Ca}^{2+}$  responses showed significantly larger than the average values (For example:  $\Delta F/F=1.54$  compared  $\Delta F/F=0.2$ ).

### Puff-application of Glu evoked $\text{Ca}^{2+}$ signals

Glu  $\alpha$ -amino-3-hydroxy-5-methyl-4-isoxazole-propionic acid (AMPA) can contribute to calcium influx.<sup>13,39</sup> In this study, exogenous Glu ion channels agonist Glu (1 mM) was puff applied (10 psi, 100 ms) in the presence of picrotoxin. As shown in Figure 6(a) and (b), puff-application of Glu induced EPSC currents ( $-112.7 \pm 10.1$  pA,  $n=10$  neurons/5 mice). These currents were significantly reduced by AMPA receptor

antagonist CNQX ( $-21.6 \pm 4.9$  pA,  $P < 0.001$ ;  $18.4 \pm 3.2\%$  for control) and almost completely blocked by additional NMDA receptor antagonist AP5 ( $-11.1 \pm 2.1$  pA,  $P < 0.001$ ;  $10.0 \pm 2.3\%$  for control). At the same time, puff-application of Glu induced EPSCs associated with a remarkable subthreshold soma calcium influx ( $\Delta F/F=0.26 \pm 0.06$ ), and only a small reduction by CNQX ( $\Delta F/F=0.19 \pm 0.04$ ,  $P > 0.05$ ;  $73.6 \pm 0.4\%$  for control) even though EPSC was almost inhibited. Application of AP5 significantly reduced the  $\text{Ca}^{2+}$  signals ( $\Delta F/F=0.10 \pm 0.01$ ,  $P < 0.01$ ;  $37.9 \pm 0.1\%$  for control, Figure 6(a) and (c)).

As shown in Figure 7, puff-application of Glu also induced obvious  $\text{Ca}^{2+}$  signals in spines, but not all spines had detectable signals. We found that there were 61.9% responses of spines after puff-application of Glu (13 spines in total 21 spines/6 neurons) (Figure 7(c)).

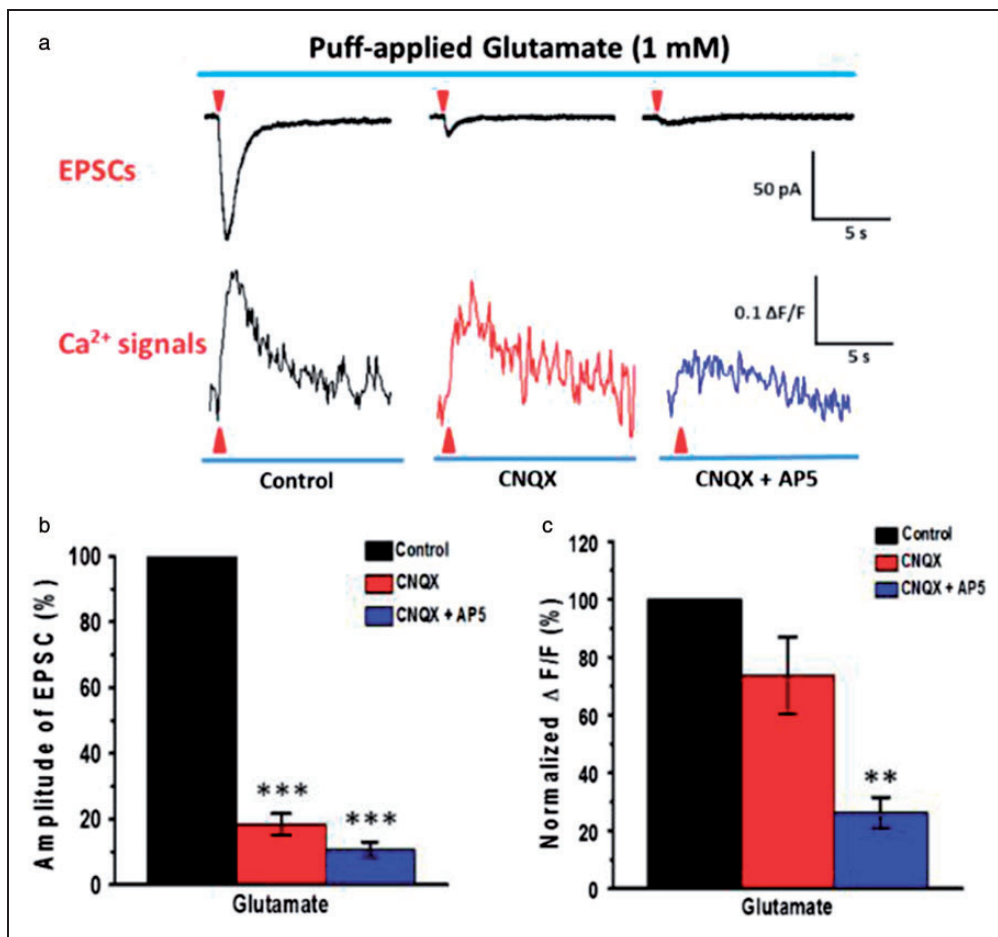


**Figure 6.** NMDA receptors-mediated puff-application of Glu evoked  $\text{Ca}^{2+}$  signal in soma of ACC pyramidal neurons. (a) Average traces of EPSCs (upper) and associated  $\text{Ca}^{2+}$  signals ( $\Delta F/F$ ) (down) evoked by puff-application of 1 mM Glu (10 psi, 100 ms,  $n=6$  neurons from 3 mice). (b) and (c) Summary results showing the percentage of EPSCs and  $\text{Ca}^{2+}$  signals ( $\Delta F/F$ ) in the presence of CNQX (20  $\mu\text{M}$ ) and AP5 (50  $\mu\text{M}$ ).  $**P < 0.01$  and  $***P < 0.001$ , error bars indicated SEM. The amplitudes of EPSCs and associated  $\text{Ca}^{2+}$  signals ( $\Delta F/F$ ) were normalized to control values.



Consistent with soma  $\text{Ca}^{2+}$  signals, the signals of spines after puff-application of Glu ( $\Delta\text{F}/\text{F} = 0.27 \pm 0.07$ ) were slightly decreased by CNQX ( $\Delta\text{F}/\text{F} = 0.18 \pm 0.02$ ,  $P > 0.05$ ;  $67.3 \pm 9.1\%$  for control) and almost abolished by additional AP5 ( $\Delta\text{F}/\text{F} = 0.07 \pm 0.01$ ,  $P < 0.05$ ;  $24.8 \pm 3.7\%$  for control) (Figure 7(a), (b), and (d)). Together, these results suggest that puff-application of Glu can evoke robustly subthreshold  $\text{Ca}^{2+}$  signals that are mediated by NMDA receptors in the somas and spines of ACC pyramidal neurons.

### NMDA receptors-dependent $\text{Ca}^{2+}$ signals induced by LTP

ACC LTP is known to be calcium dependent, but no study has reported LTP induced calcium imaging directly in the ACC pyramidal neurons. In the present study, we recorded LTP-evoked  $\text{Ca}^{2+}$  signals induced by three different types of LTP induction paradigms: spike-timing, TBS, and pairing protocols. We found

that three LTP protocols can successfully induce post-LTP in ACC neurons (spike-timing:  $150.6\% \pm 9.5\%$  of baseline,  $n = 7$  neurons/3 mice; TBS:  $149.8\% \pm 16.4\%$  of baseline,  $n = 6$  neurons/3 mice; pairing:  $143.2\% \pm 7.8\%$  of baseline,  $n = 7$  neurons/3 mice; Figure 8(b)). These LTP were completely blocked by AP5 (spike-timing:  $97.2\% \pm 2.3\%$ ,  $P < 0.05$ ,  $n = 6$  neurons/3 mice; TBS:  $95.5\% \pm 5.4\%$ ,  $P < 0.05$ ,  $n = 7$  neurons/3 mice; pairing:  $100.4\% \pm 7.1\%$ ,  $P < 0.05$ ,  $n = 5$  neurons/3 mice; Figure 8(b)). These results are similar to those previously reported in our group research.<sup>7,26</sup>

We also found that there were obvious  $\text{Ca}^{2+}$  influx with different kinetics in the process of three LTP induction (Figure 8(c) and (d)). One phase of  $\text{Ca}^{2+}$  increase by three LTP protocols was shown in Figure 8(c). Spike-timing protocol produced fast remarkable  $\text{Ca}^{2+}$  transient with a short rise time and decay time. TBS protocol also induced remarkable  $\text{Ca}^{2+}$  transient with a slow rise time and decay time. After pairing protocol,  $\text{Ca}^{2+}$  influx increased slowly and had a long decay time either.

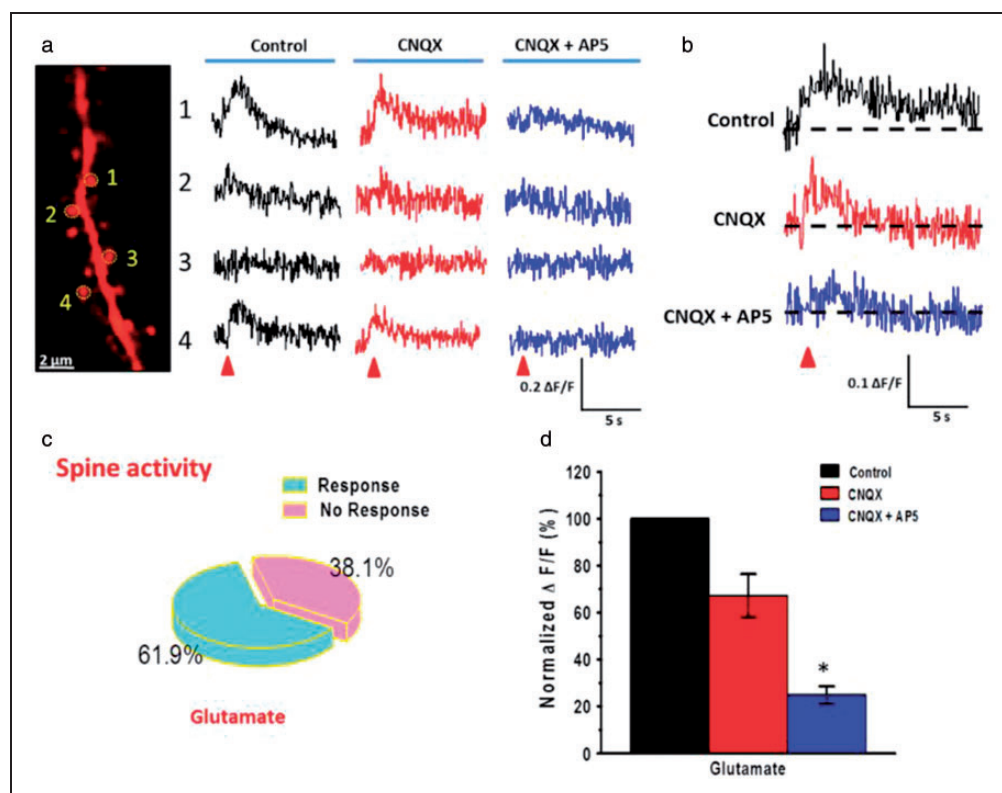


**Figure 7.** NMDA receptor-mediated puff-application of Glu evoked  $\text{Ca}^{2+}$  signal in spine of ACC pyramidal neurons. (a) Far left, two-photon fluorescent image of a dendritic segment containing active spines. The yellow dashed circles indicate the position of the frame scan. Right, four spines representative calcium transients waveforms of fluorescence changes ( $\Delta\text{F}/\text{F}$ ) in response to puff-application of 1 mM Glu (10 psi, 100 ms) in the control, CNQX, and CNQX + AP5 conditions, respectively. (b) Average traces of  $\text{Ca}^{2+}$  signals ( $\Delta\text{F}/\text{F}$ ) in responsive spines evoked by puff-application of Glu in the control ACSF, presence of CNQX (20  $\mu\text{M}$ ), and AP5 (50  $\mu\text{M}$ ), respectively. (c) Pie graph showing the percentage of active spines in the puff-application of Glu. (d) Summary results showing the percentage of  $\text{Ca}^{2+}$  signals ( $\Delta\text{F}/\text{F}$ ) in responsive spines in the presence of CNQX and AP5. \* $P < 0.05$ , error bars indicated SEM. The amplitudes of  $\text{Ca}^{2+}$  signals ( $\Delta\text{F}/\text{F}$ ) were normalized to control values.

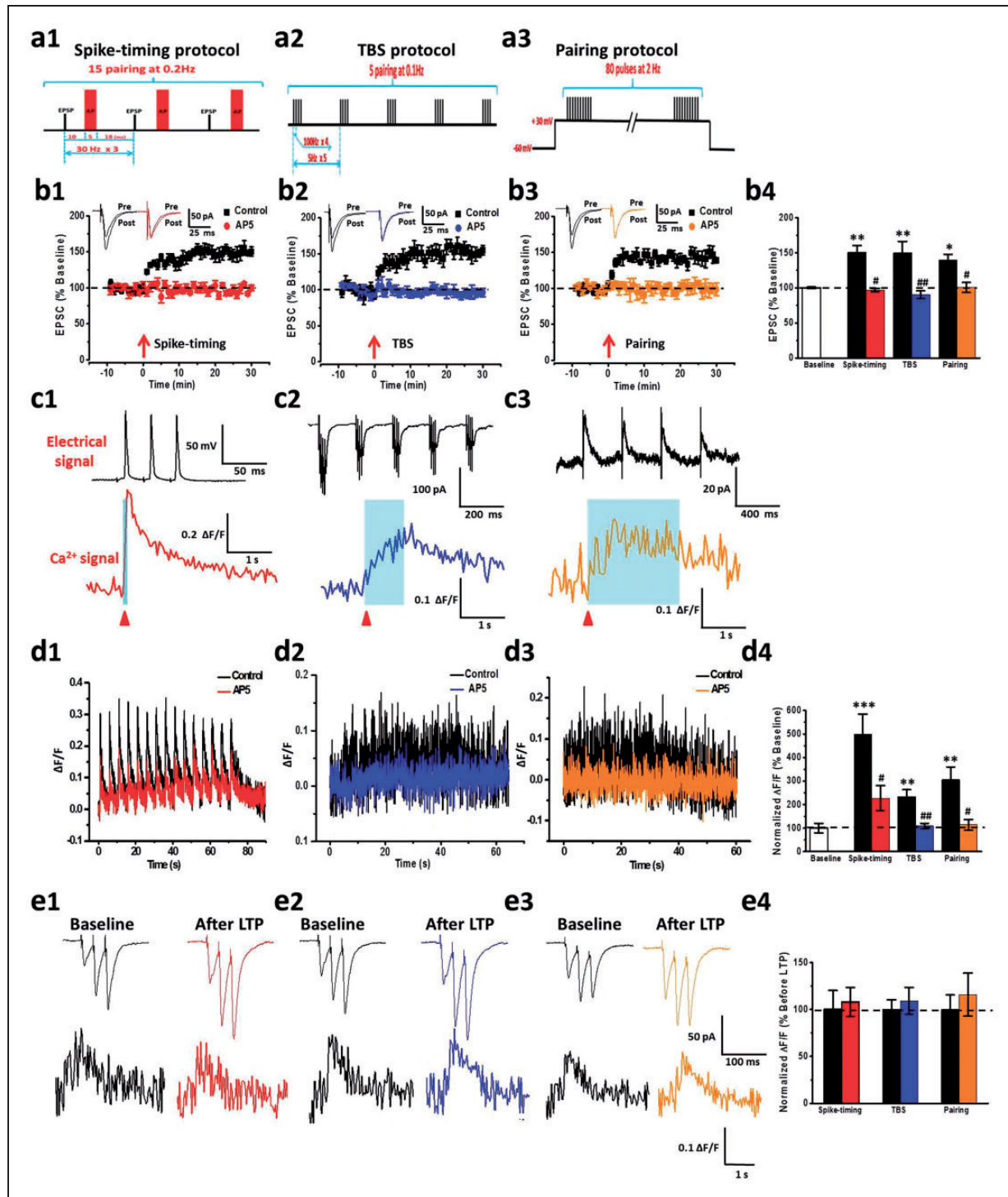


**Figure 8.** Three kinds of LTP induction paradigms evoked NMDA receptor-dependent  $\text{Ca}^{2+}$  signals in ACC pyramidal neurons. (a) Schematic diagrams showing the spike-timing (a1), TBS (a2), and pairing (a3) LTP induction paradigms. (b) LTP was induced by spike-timing, TBS, and pairing protocols, and AP5 blocked three kinds of LTP from left to right sides, respectively. Summary results showed the effects of three types of LTP induction paradigms and AP5 on LTP (b4). The arrows denote the time of LTP induction. The dashed line indicates the mean basal synaptic responses. (c) Representative traces of electric signals (upper) and associated  $\text{Ca}^{2+}$  signals ( $\Delta\text{F}/\text{F}$ ) (down) evoked by one pulse spike-timing (c1), one pulse TBS (c2), and 2 s pairing (c3) stimulation. (d)  $\text{Ca}^{2+}$  signals of the whole process of LTP induction by spike-timing (left), TBS (middle), and pairing (right) stimulation. AP5 reduced LTP-dependent  $\text{Ca}^{2+}$  signals. Summary results showed the  $\text{Ca}^{2+}$  signals in whole process of LTP induction by three kinds of paradigms and the effects of AP5 on them (d4). (e) Representative traces of three stimuli at 50 Hz induced EPSCs (upper) and associated  $\text{Ca}^{2+}$  signals ( $\Delta\text{F}/\text{F}$ ) (down) in baseline and 30 min after LTP stimulation. Summary results showed the  $\text{Ca}^{2+}$  signals in baseline and 30 min after LTP stimulation by three types of paradigms (e4). All red arrowheads mark the time points of synaptic stimulation. \* $p < 0.05$ , \*\* $p < 0.01$ , and \*\*\* $p < 0.001$ , error bars indicated SEM. The amplitudes of  $\text{Ca}^{2+}$  signals ( $\Delta\text{F}/\text{F}$ ) were normalized to control values. LTP: long-term potentiation.

The amplitude of  $\text{Ca}^{2+}$  influx induced by pairing protocol increased larger than TBS protocol induced but smaller than spike-timing protocol induced. In the whole process of LTP induction (Figure 8(d)), spike-timing protocol induced 15 spikes fast  $\text{Ca}^{2+}$  influxes and lasted 75 s ( $\Delta\text{F}/\text{F} = 0.38 \pm 0.09$ ,  $442.6\% \pm 108.1\%$  of baseline,  $P < 0.05$ ).  $\text{Ca}^{2+}$  signals induced by TBS protocol increased gradually and had a summation property with stimulation ( $\Delta\text{F}/\text{F} = 0.23 \pm 0.03$ ,  $269.5\% \pm 30.5\%$  of baseline,  $P < 0.05$ ). However, the  $\text{Ca}^{2+}$  signals induced by pairing protocol reached the peak after 20 s of induction and kept stable ( $\Delta\text{F}/\text{F} = 0.30 \pm 0.05$ ,  $347.1\% \pm 60.1\%$  of baseline,  $P < 0.05$ ). We then evaluated the contributions of NMDA receptors on LTP-induced  $\text{Ca}^{2+}$  signals. We found that NMDA receptor mediated the  $\text{Ca}^{2+}$  signals induced by three LTP protocols with a much different manner in kinetics. Spike-timing protocol-induced  $\text{Ca}^{2+}$  signals were reduced by AP5 ( $\Delta\text{F}/\text{F} = 0.22 \pm 0.05$ ,  $257.6\% \pm 60.1\%$  of baseline,  $P < 0.05$ ; Figure 8(d1)). AP5 almost completely inhibited  $\text{Ca}^{2+}$  signals that were evoked by both TBS and pairing protocols (TBS:  $\Delta\text{F}/\text{F} = 0.11 \pm 0.01$ ,  $124.0\% \pm 12.7\%$  of baseline,  $P < 0.05$ , Figure 8(d2) and (d4); pairing:  $\Delta\text{F}/\text{F} = 0.11 \pm 0.02$ ,  $129.2\% \pm 25.9\%$  of baseline,  $P < 0.05$ ; Figure 8(d3) and (d4)).

In addition, we want to know whether the basal  $\text{Ca}^{2+}$  signal is changed during LTP. To address this problem, three electrical stimuli at 50 Hz were triggered to evoke synaptic responses before and after 30 min LTP induction. As shown in Figure 8(e), there were no significant changes for  $\text{Ca}^{2+}$  signals before and after LTP induction.

## Discussion

Calcium influx is thought to be critical for synaptic transmission and plasticity. Our previous studies show that  $\text{Ca}^{2+}$ -dependent biochemical cascades are important for ACC LTP as well as injury-triggered synaptic changes in the ACC.<sup>1,2,7</sup> Our present results show for the first time that NMDA receptors contribute to postsynaptic calcium influx triggered by LTP in ACC pyramidal neurons. This finding further supports our current hypothesis that NMDA receptor-dependent calcium signaling pathways are important for synaptic plasticity in ACC and behavioral sensitization.<sup>2,5,7</sup>

APs of neurons can precisely control information transmission.<sup>40,41</sup> We found that APs evoked significant suprathreshold  $\text{Ca}^{2+}$  signals and have summation properties in the soma and dendritic spine of ACC pyramidal neurons. Subthreshold stimulation that induced synaptic responses (i.e., eEPSCs) also evoked  $\text{Ca}^{2+}$  influx. Furthermore, single subthreshold stimulation did not induce reliable  $\text{Ca}^{2+}$  signal. Only repetitive electrical stimulation (50 Hz for three traces) induced weak  $\text{Ca}^{2+}$  signals. This is similar to a previous report in the hippocampus.<sup>17</sup>

NMDA receptors are believed to be essential for  $\text{Ca}^{2+}$  influx in the ACC. Here, we find NMDA receptors contribute to  $\text{Ca}^{2+}$  signaling induced by APs, eEPSCs, and LTP inducing protocol in ACC pyramidal neurons. In the hippocampus, previous reports have been reported that suprathreshold  $\text{Ca}^{2+}$  signals are mainly mediated by VGCCs.<sup>17,38,41,42</sup> However, a recent study in the hippocampus show that NMDA receptor mediate both suprathreshold and subthreshold  $\text{Ca}^{2+}$  signals. They showed that suprathreshold stimulation-activated NMDA receptor induced  $\text{Ca}^{2+}$  influx and burst firing evoked multi-dendrite  $\text{Ca}^{2+}$  spikes were dependent on NMDA receptors in the hippocampus.<sup>10</sup> In addition, NMDA receptors have been reported to AP-evoked  $\text{Ca}^{2+}$  signals in pyramidal cell terminals.<sup>43</sup> In the present study, CNQX blocked the puff-application induced eEPSCs but slightly reduced associated  $\text{Ca}^{2+}$  signals. In addition, we found that puff-application of NMDA evoked almost three folds  $\text{Ca}^{2+}$  signals than puff-application of Glu in both soma and spine of the ACC neurons (unpublished data). These results strongly support that NMDA receptors are essential for  $\text{Ca}^{2+}$  influx in ACC neurons.

LTP is a major form of synaptic plasticity in ACC. We find that LTP induction protocols, including spike-timing, TBS, and pairing LTP, can induce calcium influx. These  $\text{Ca}^{2+}$  signals all require the activation of NMDA receptors. This finding is similar to that in hippocampus.<sup>19,44,45</sup> We also find that the three protocols trigger an increase in  $\text{Ca}^{2+}$  signals with different kinetics. It is possible that various calcium signal patterns caused by different LTP inducing protocols may contribute potential different intracellular mechanisms. It is also unclear that suprathreshold and subthreshold calcium signals play different roles in ACC synaptic plasticity. The involvement of VGCCs in ACC LTP depends on the recording methods. LTP recorded using whole-cell patch-recording method is not blocked by nimodipine (unpublished observation). By contrast, LTP recorded using field EPSPs is sensitive to nifedipine.<sup>46</sup> These results suggest that different induction protocols may activate different receptors/ion channels for  $\text{Ca}^{2+}$  ions influx in the ACC.<sup>47</sup> In consistent with this speculation, it has been reported that different LTP induction protocols activate distinct signaling pathways that produced LTP with different expression mechanisms in hippocampus.<sup>47,48</sup> In the present study, we performed imaging of the soma and spine  $\text{Ca}^{2+}$  separately. It will be useful in future studies to imaging them simultaneously and compare their time courses. Furthermore, intracellular signaling pathways linked to  $\text{Ca}^{2+}$  signaling in the soma and spine may be different.

ACC LTP is believed to be the key mechanism for pain-mediated synaptic plasticity. The postsynaptic  $\text{Ca}^{2+}$  serves as an important intracellular signal for triggering a series of biochemical events that contribute to

the expression of LTP for chronic pain. Our previous studies also show that calcium-stimulated signaling pathways are very important for chronic pain.<sup>5,7,39,49</sup> Our present study provides strong evidence to support the hypothesis that activation of NMDA receptors leads to an increase in postsynaptic Ca<sup>2+</sup> signals in ACC neurons. Therefore, studying the Ca<sup>2+</sup> signals in ACC can help to understand the mechanisms of chronic pain. Future studies are clearly needed to investigate the properties of Ca<sup>2+</sup> signals in chronic pain conditions and potential roles of different NMDA receptor subtypes for Ca<sup>2+</sup> signals.

### Acknowledgment

The authors would like to thank Melissa Lepp and Rongfeng Hu for English editing.

### Author Contributions

XHL, TC, and MZ designed the experiments. XHL and QS performed experiments and analyzed data; XHL, TC, and MZ drafted the manuscript and finished the final vision of the manuscript. All authors read and approved the final manuscript.

### Declaration of Conflicting Interests

The author(s) declared no potential conflicts of interest with respect to the research, authorship, and/or publication of this article.

### Funding

The author(s) disclosed receipt of the following financial support for the research, authorship, and/or publication of this article: This work was supported by grants from the Canadian Institute for Health Research (CIHR) Michael Smith Chair in Neurosciences and Mental Health, Canada Research Chair, CIHR operating grant (MOP-124807), and project grant (PJT-148648), Azrieli Neurodevelopmental Research Program and Brain Canada awarded to MZ and National Natural Science Foundation of China (31371126 and 81671095) to TC.

### References

- Zhuo M. Neural mechanisms underlying anxiety-chronic pain interactions. *Trends Neurosci* 2016; 39: 136–145.
- Bliss TV, Collingridge GL, Kaang BK, et al. Synaptic plasticity in the anterior cingulate cortex in acute and chronic pain. *Nat Rev Neurosci* 2016; 17: 485–496.
- Kandel ER. The molecular biology of memory: cAMP, PKA, CRE, CREB-1, CREB-2, and CPEB. *Mol Brain* 2012; 5: 14.
- Ghosh A and Giese KP. Calcium/calmodulin-dependent kinase II and Alzheimer's disease. *Mol Brain* 2015; 8: 78.
- Zhuo M. Long-term potentiation in the anterior cingulate cortex and chronic pain. *Philos Trans R Soc London Ser B, Biol Sci* 2014; 369: 20130146.
- Sanhueza M and Lisman J. The CaMKII/NMDAR complex as a molecular memory. *Mol Brain* 2013; 6: 10.
- Zhuo M. Cortical excitation and chronic pain. *Trends Neurosci* 2008; 31: 199–207.
- Leitner FC, Melzer S, Lutcke H, et al. Spatially segregated feedforward and feedback neurons support differential odor processing in the lateral entorhinal cortex. *Nat Neurosci* 2016; 19: 935–944.
- Segal M and Korkotian E. Roles of calcium stores and store-operated channels in plasticity of dendritic spines. *Neuroscientist* 2015; 22: 477–485.
- Grienberger C, Chen X and Konnerth A. NMDA receptor-dependent multidendrite Ca(2+) spikes required for hippocampal burst firing in vivo. *Neuron* 2014; 81: 1274–1281.
- Marlin JJ and Carter AG. GABA-A receptor inhibition of local calcium signaling in spines and dendrites. *J Neurosci* 2014; 34: 15898–15911.
- Parent MA, Wang L, Su J, et al. Identification of the hippocampal input to medial prefrontal cortex in vitro. *Cereb Cortex* 2010; 20: 393–403.
- Grienberger C and Konnerth A. Imaging calcium in neurons. *Neuron* 2012; 73: 862–885.
- Segal M and Korkotian E. Roles of calcium stores and store-operated channels in plasticity of dendritic spines. *Neuroscientist* 2016; 22: 477–485.
- Agostini M and Fasolato C. When, where and how? Focus on neuronal calcium dysfunctions in Alzheimer's disease. *Cell Calcium* 2016; 60: 289–298.
- Metz AE, Jarsky T, Martina M, et al. R-type calcium channels contribute to afterdepolarization and bursting in hippocampal CA1 pyramidal neurons. *J Neurosci* 2005; 25: 5763–5773.
- Kovalchuk Y, Eilers J, Lisman J, et al. NMDA receptor-mediated subthreshold Ca(2+) signals in spines of hippocampal neurons. *J Neurosci* 2000; 20: 1791–1799.
- Lee KF, Soares C, Thivierge JP, et al. Correlated synaptic inputs drive dendritic calcium amplification and cooperative plasticity during clustered synapse development. *Neuron* 2016; 89: 784–799.
- Zhang XH, Wu LJ, Gong B, et al. Induction- and conditioning-protocol dependent involvement of NR2B-containing NMDA receptors in synaptic potentiation and contextual fear memory in the hippocampal CA1 region of rats. *Mol Brain* 2008; 1: 9.
- Koga K, Descalzi G, Chen T, et al. Coexistence of two forms of LTP in ACC provides a synaptic mechanism for the interactions between anxiety and chronic pain. *Neuron* 2015; 85: 377–389.
- Liu SB, Zhang MM, Cheng LF, et al. Long-term upregulation of cortical glutamatergic AMPA receptors in a mouse model of chronic visceral pain. *Mol Brain* 2015; 8: 76.
- Chen T, Wang W, Dong YL, et al. Postsynaptic insertion of AMPA receptor onto cortical pyramidal neurons in the anterior cingulate cortex after peripheral nerve injury. *Mol Brain* 2014; 7: 76.
- Li XY, Ko HG, Chen T, et al. Alleviating neuropathic pain hypersensitivity by inhibiting PKMzeta in the anterior cingulate cortex. *Science* 2010; 330: 1400–1414.
- Xu H, Wu LJ, Wang H, et al. Presynaptic and postsynaptic amplifications of neuropathic pain in the anterior cingulate cortex. *J Neurosci* 2008; 28: 7445–7453.

25. Wang H, Wu LJ, Zhang F, et al. Roles of calcium-stimulated adenylyl cyclase and calmodulin-dependent protein kinase IV in the regulation of FMRP by group I metabotropic glutamate receptors. *J Neurosci* 2008; 28: 4385–4397.
26. Zhao MG, Toyoda H, Lee YS, et al. Roles of NMDA NR2B subtype receptor in prefrontal long-term potentiation and contextual fear memory. *Neuron* 2005; 47: 859–872.
27. Wei F, Xia XM, Tang J, et al. Calmodulin regulates synaptic plasticity in the anterior cingulate cortex and behavioral responses: a microelectroporation study in adult rodents. *J Neurosci* 2003; 23: 8402–8409.
28. Sheffield ME and Dombeck DA. Calcium transient prevalence across the dendritic arbour predicts place field properties. *Nature* 2015; 517: 200–214.
29. Chen T, Koga K, Descalzi G, et al. Postsynaptic potentiation of corticospinal projecting neurons in the anterior cingulate cortex after nerve injury. *Mol Pain* 2014; 10: 33.
30. Yamanaka M, Tian Z, Darvish-Ghane S, et al. Pre-LTP requires extracellular signal-regulated kinase in the ACC. *Mol Pain* 2016; 12: 1744806916647373.
31. Darvish-Ghane S, Yamanaka M and Zhuo M. Dopaminergic modulation of excitatory transmission in the anterior cingulate cortex of adult mice. *Mol Pain* 2016; 12: 1744806916648153.
32. Lock JT, Parker I and Smith IF. A comparison of fluorescent Ca(2)(+) indicators for imaging local Ca(2)(+) signals in cultured cells. *Cell Calcium* 2015; 58: 638–648.
33. Tada M, Takeuchi A, Hashizume M, et al. A highly sensitive fluorescent indicator dye for calcium imaging of neural activity in vitro and in vivo. *Eur J Neurosci* 2014; 39: 1720–1728.
34. Wu LJ, Zhao MG, Toyoda H, et al. Kainate receptor-mediated synaptic transmission in the adult anterior cingulate cortex. *J Neurophysiol* 2005; 94: 1805–1813.
35. Araya R, Vogels TP and Yuste R. Activity-dependent dendritic spine neck changes are correlated with synaptic strength. *Proc Natl Acad Sci U S A* 2014; 111: E2895–E2904.
36. Wilson JM, Dombeck DA, Diaz-Rios M, et al. Two-photon calcium imaging of network activity in XFP-expressing neurons in the mouse. *J Neurophysiol* 2007; 97: 3118–3125.
37. Tsvetkov E, Carlezon WA, Benes FM, et al. Fear conditioning occludes LTP-induced presynaptic enhancement of synaptic transmission in the cortical pathway to the lateral amygdala. *Neuron* 2002; 34: 289–300.
38. Schiller J, Major G, Koester HJ, et al. NMDA spikes in basal dendrites of cortical pyramidal neurons. *Nature* 2000; 404: 285–289.
39. Zhuo M. Ionotropic glutamate receptors contribute to pain transmission and chronic pain. *Neuropharmacology* 2017; 112: 228–234.
40. Hage TA and Khaliq ZM. Tonic firing rate controls dendritic Ca2+ signaling and synaptic gain in substantia nigra dopamine neurons. *J Neurosci* 2015; 35: 5823–5836.
41. Waters J, Schaefer A and Sakmann B. Backpropagating action potentials in neurons: measurement, mechanisms and potential functions. *Prog Biophys Mol Biol* 2005; 87: 145–170.
42. Bloodgood BL and Sabatini BL. Ca(2+) signaling in dendritic spines. *Curr Opin Neurobiol* 2007; 17: 345–351.
43. Buchanan KA, Blackman AV, Moreau AW, et al. Target-specific expression of presynaptic NMDA receptors in neocortical microcircuits. *Neuron* 2012; 75: 451–466.
44. Bliss TV and Collingridge GL. Expression of NMDA receptor-dependent LTP in the hippocampus: bridging the divide. *Mol Brain* 2013; 6: 5.
45. Bliss TV and Collingridge GL. A synaptic model of memory: long-term potentiation in the hippocampus. *Nature* 1993; 361: 31–39.
46. Kang SJ, Liu MG, Shi TY, et al. N-type voltage gated calcium channels mediate excitatory synaptic transmission in the anterior cingulate cortex of adult mice. *Mol Pain* 2013; 9: 58.
47. Lisman J. Long-term potentiation: outstanding questions and attempted synthesis. *Philos Trans R Soc London Ser B, Biol Sci* 2003; 358: 829–842.
48. Hoffman DA, Sprengel R and Sakmann B. Molecular dissection of hippocampal theta-burst pairing potentiation. *Proc Natl Acad Sci U S A* 2002; 99: 7740–7745.
49. Zhuo M. Contribution of synaptic plasticity in the insular cortex to chronic pain. *Neuroscience* 2016; 338: 220–229.